International Journal of Innovative Research and Scientific Studies, 9(1) 2026, pages: 59-70

ISSN: 2617-6548

URL: www.ijirss.com

Learning finger movement patterns for a transradial prosthesis using artificial neural networks

Jesus de la Cruz-Alejo[1*], Belem Arce-Vazquez[2], Hugo Beatriz-Cuellar[1], Agustín Mora-Ortega[1], Jesus Antonio Lobato-Cadena[3]

[1]*Tecnologico Nacional de México, Tecnológico de Estudios Superiores de Ecatepec, Estado de México, México.*
[2]*Universidad Autónoma Metropolitana Unidad Lerma, División de Ciencias Biológicas y de la Salud, México.*
[3]*Instituto Politécnico Nacional, ESIME Azcapotzalco, México.*

Corresponding author: Jesus de la Cruz-Alejo (*Email: jdelacruz@tese.edu.mx*)

Abstract

This article presents an approach to achieving flexibility in a transradial prosthesis that allows the grasping of objects of different shapes through a hardware-implemented control architecture, enabling users to perform various activities of daily living. The proposed generalized hardware architecture utilizes an artificial neural network, facilitating the adjustment and interconnection between neurons, as well as providing adequate resolution to adapt the behavior to diverse finger movement patterns. To this end, distance sensors were incorporated into the prosthesis fingers to obtain information about the distance to objects. Servomotors were also used to manipulate the position of the fingers based on the data obtained from the sensors. A central composite design was used to train the network to identify finger movement patterns, generating appropriate combinations of independent variables (sensor data) and their association with their respective responses (motor movements). The main result of this proposal is that the assumption of the values assigned to the patterns is matched by the prosthesis through the gripping and holding of cylindrical, spherical and rectangular objects with an accuracy of 97.8%, a mean square error of 1.7042° and a response time of 0.5 seconds.

Keywords: Artificial neural network, Identification, Patterns, Transradial prosthesis.

DOI: 10.53894/ijirss.v9i1.11156
Funding: This research was supported by the Secretaría de Ciencia, Humanidades, Tecnología e Innovación (SECIHTI) through graduate scholarships awarded to Hugo Beatriz Cuellar (CVU: 1007017) and Jesús Antonio Lobato Cadena (CVU: 1195239). Additional financial support was provided by the Tecnológico Nacional de México (TECNM) for the project entitled “Design and implementation of an intelligent control system applied to a superior ergonomic transradial prosthesis for the rehabilitation of people” (Project ID: 21673.25-PD).
History: Received: 17 November 2025 / **Revised:** 25 December 2025 / **Accepted:** 30 December 2025 / **Published:** 9 January 2026

Competing Interests: The authors declare that they have no competing interests.
Authors’ Contributions: All authors contributed equally to the conception and design of the study. All authors have read and agreed to the published version of the manuscript.
Transparency: The authors confirm that the manuscript is an honest, accurate, and transparent account of the study; that no vital features of the study have been omitted; and that any discrepancies from the study as planned have been explained. This study followed all ethical practices during writing.
Publisher: Innovative Research Publishing

1. Introduction

In recent years, there has been a growing interest in improving the quality of life for people with disabilities. In this context, motor disability due to the absence of an arm at the transradial level can cause functional limitations such as difficulty manipulating and grasping objects, changes in body biomechanics, limited employment opportunities, psychological problems, and difficulty performing daily activities [1, 2]. Today, active, myoelectric, hybrid, bionic, and intelligent prostheses are available as alternatives to replace a forearm and allow a person to resume some of their daily activities. However, most commercially available transradial prosthesis designs are expensive, difficult to design and control, have poor aesthetics, and slow operating speed, among other limitations [3-7]. For this reason, the design and development of low-cost transradial prostheses that allow for a wide variety of movements with high precision and rapid response are required. In this regard, several studies have been conducted on transradial prostheses, such as Prakash and Sharma [8] which presents a 3D-printed transradial prosthesis controlled by muscle contractions detected by an EMG sensor and a closed-loop position control system to manage its operation [9] presented a 3D-printed transradial prosthesis controlled with an Arduino board and six servomotors, used to measure the accuracy of finger positioning, specifically the angles of the distal phalanges. Fang, et al. [10] presented a method for the simultaneous recognition of gestures and forces for interaction with a prosthetic hand. This involves collecting data using EMG and force sensors, which are then fed into a convolutional neural network for training. Furthermore, the prosthetic hand has six degrees of freedom, and each fingertip incorporates tactile sensors that allow for the implementation of three levels of grip strength. Furthermore, transradial prostheses are composed of various components (socket, control system, terminal unit, etc.), employ different types of sensors and actuators (servomotors, linear actuators, myoelectric sensors, force sensors, position sensors, etc.), and utilize diverse control systems (myoelectric, electromyographic, artificial neural networks, fuzzy logic, etc.). However, a sufficiently precise system for detecting arm muscle movements has not yet been developed, highly accurate control has not been implemented, and the prosthesis's aesthetics need improvement. Additionally, devices that use electromyographic signals require a lengthy user training period, depend heavily on the robustness of these signals, and generally perform tasks involving grasping symmetrical objects [11, 12]. Another relevant aspect is the number and type of movements that these prostheses can perform, as this factor is crucial before, during and after the development of these devices.

Based on the above, the objective of this work is the design and construction of a transradial prosthesis for gripping objects of different shapes (circular, cylindrical, rectangular, spherical, etc.). To achieve this, distance sensors placed on the five fingers were used to obtain data on the object's shape characteristics. Five servomotors and nylon thread were used to adjust the finger position. An artificial neural network (ANN) was designed to identify the patterns that describe the object's shape and determine the type of grip. A central composite design (CCD) was used to configure the samples or patterns used for training the ANN. An Arduino Mega 2560 board was also used to implement the ANN algorithm for prosthesis control, and to acquire the sensor signals and produce the control signals to adjust the actuator position. An artificial neural network was used because it is a computational model inspired by the functioning of the human brain and can be implemented in various programming languages, facilitating its integration into software and hardware systems. Furthermore, artificial neural networks have demonstrated a wide range of applications in diverse fields, such as systems optimization [13, 14] medical applications [15] prediction of electrical energy production [16, 17] and biotechnological processes [18, 19] among others. With the development of this project, it is hoped to contribute to the development of more effective prostheses with a greater number of functions than most current prostheses, which can perform finger gestures and open and close the fingers to grasp objects. The structure of this scientific article is as follows: section two describes each of the elements used in the development of the prosthesis, section three shows the results obtained from the simulation of the system, section four shows the experimental tests and validation of the proposed prosthesis, and section five presents the conclusions obtained of the work.

2. Description of the Operation of the Transradial Prosthesis

Figure 1 shows a block diagram representing the structure of the system used to control the operation of the transradial prosthesis. In this system, five servomotors (SM1, SM2, SM3, SM4, and SM5) were used to move the five fingers of the prosthesis. Five distance sensors (DS1, DS2, DS3, DS4, and DS5) were used to obtain data characterizing the shape of objects. An artificial neural network was used to identify the object's shape from the data obtained by the sensors and determine the appropriate actuator movement to grasp it. In this context, the artificial neural network is responsible for pattern recognition; that is, it determines the common characteristics among different object shapes. To correctly grasp an object and prevent it from shifting or falling due to differences in distance between the fingers and the object, the appropriate speed for each servomotor is calculated. For this project, rotary actuators were chosen because they offer a fast response and high positioning accuracy, allow for speed control, can maintain a fixed position, and provide high torque, among other advantages. Distance sensors were also selected instead of myoelectric sensors because myoelectric signals have several disadvantages. For example, interpretation is difficult due to electrical noise and interference from other muscles, signal processing is complex, prolonged use can cause discomfort, and they require very precise placement, among other drawbacks. In contrast, distance sensors do not present these difficulties, as they interact directly with the object, and their response is easy to acquire and interpret.

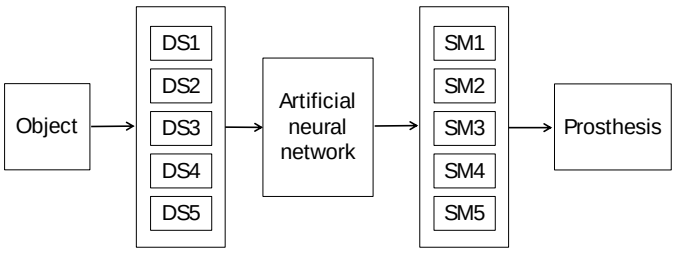

Figure 1.
Block diagram of the transradial prosthesis.

2.1. Mechanical Design of the Transradial Prosthesis

Figures 2(a), 2(b), and 2(c) show the proposed design for the prosthesis. Figures 3(a) and 3(b) depict the mechanical system used to generate finger movement in the transradial prosthesis. As can be seen, distance sensors were placed on the fingers, and each finger is moved by a servomotor and a nylon thread, which simulates the tendons of the human hand. In this case, the nylon thread is connected from the fingertip to the forearm, passing through a set of guides before reaching the servomotor. The rotation of the servomotor winds the thread, causing the finger to flex. Finally, a spring was placed in the joint of each finger to return it to its initial position once the servomotor movement is complete. This position is the fully open hand or the servomotor's zero-degree angle. The most relevant features of the proposed transradial prosthesis include ten degrees of freedom, which gives it great versatility for gripping objects of different shapes. The structure weighs 1.5 kg and is capable of handling objects up to 9 cm wide and 500 g in weight.

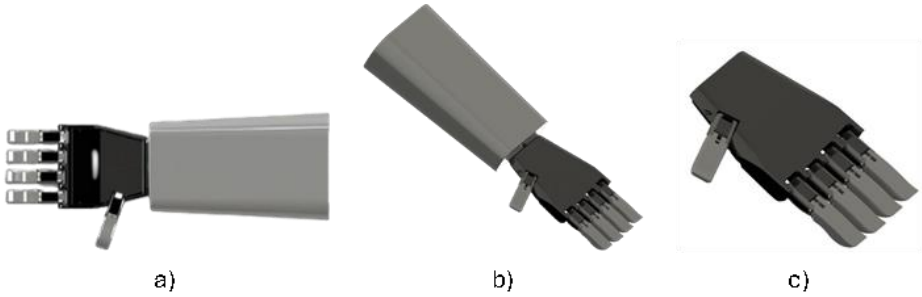

Figure 2.
Design of the transradial prosthesis, a) isometric view with socket, b) isometric view and c) top view.

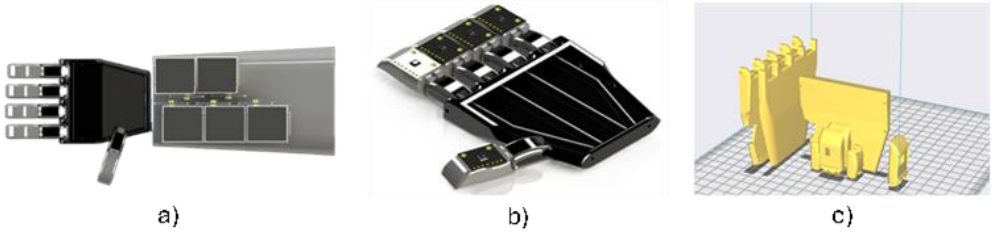

Figure 3.
Mechanical system of the transradial prosthesis, a) location of the servomotors, b) location of the sensors and nylon threads and c) printing of the prosthesis parts.

The prosthesis was manufactured using 3D printing with PLA carbon fiber, a rigid and strong material with a good strength-to-weight ratio, high wear resistance, and an attractive surface finish, among other properties. Specifically, this material has a tensile strength of 70 MPa, an elastic modulus of 7 GPa, a flexural strength of 100 MPa, and a flexural modulus of 6320 MPa. For manufacturing, a Creality CR-5 Pro H 3D printer was used with a 77% infill setting, a line pattern, and a layer height of 0.12 mm. Figure 3(c) shows the printing configuration for the mechanical parts (total weight of 150 g).

To verify the prosthesis's behavior under the action of forces during its operation, a stress analysis was performed. This analysis allows for the identification of critical failure points, the prevention of structural damage, the simulation of the structure's behavior and deformation under different loads, and the determination of the material's maximum strength. The analysis was performed using SolidWorks, a computer-aided design software that allows for 3D modeling of parts, the generation of 2D drawings, and the performance of structural and motion simulations. Figure 4(a) shows the back of the prosthesis, which has a fixed portion indicated by green arrows, while the pink arrows represent the application of a 100 N transverse load. As can be seen in Figure 4(b), the back of the prosthesis does not present a risk of breakage under this force, which is indicated by areas colored red and which are not present in the figure. However, a slight displacement of 6.728×10^{-3} mm and a maximum tension of 1.152×10^{6} N/m² were observed. On the other hand, Figure 4(c) shows one of the prosthetic fingers, to which a maximum force of 20 N was applied, due to its lower structural resistance, as its interior is hollow to allow the passage of the nylon thread. Finally, Figure 4(d) shows that the fingers also do not present a risk of

breakage under these conditions, registering a maximum displacement of 1.0745×10^{-4} mm and a tension of 2.327×10^{5} N/m².

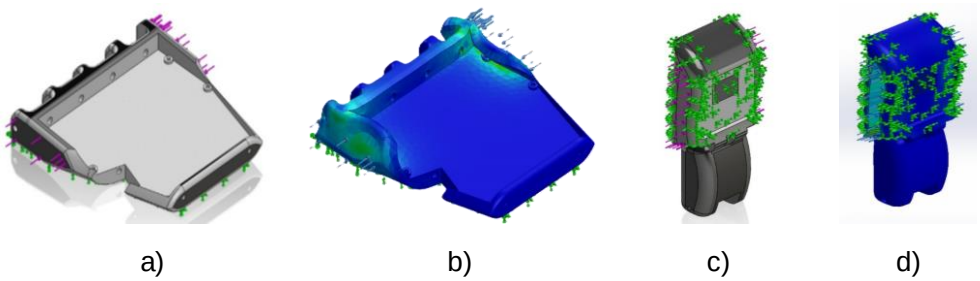

Figure 4.
Results of the stress analysis of the parts of the transradial prosthesis.

Based on the above, it is concluded that PLA carbon fiber adequately withstands the applied loads, exhibits minimal and acceptable deformation, and shows no critical stress concentrations. These results validate both the choice of material and the proposed design for the prosthesis. Figure 5 shows the constructed prototype of the prosthesis, which has a black acrylic paint finish. The mechanical parts were assembled with screws and wire to improve fastening, and the nylon thread is located on the inside to enhance the prototype's aesthetics.

Figure 5.
Transradial prosthesis prototype.

2.2. Diseño Electrónico De La Prótesis Transradial

Figure 6 shows the electronic diagram used to control the operation of the transradial prosthesis. As can be seen, an Arduino MEGA 2560 board was used to read the signals generated by the VL6180X distance sensors, denoted as S1, S2, S3, S4, and S5, which were connected to the board's analog inputs. This same board was used to implement the artificial neural network algorithm to provide control signals to the MG995 servomotors, identified as M1, M2, M3, M4, and M5, through the digital outputs. A potentiometer was also included in the electronic circuit to simulate the behavior of the distance sensors. The most relevant technical characteristics of the Arduino MEGA 2560 board are: a 5V operating voltage, 16 analog inputs, 54 digital pins, a 16 MHz clock speed, 256 KB of Flash memory, and C++ programming language, among others. These specifications make this board an accessible, low-cost option with suitable technical capabilities for this project [20-22]. Finally, a battery was used to power the electronic system, and the Arduino MEGA 2560 board was configured to operate in low-power mode to extend battery life.

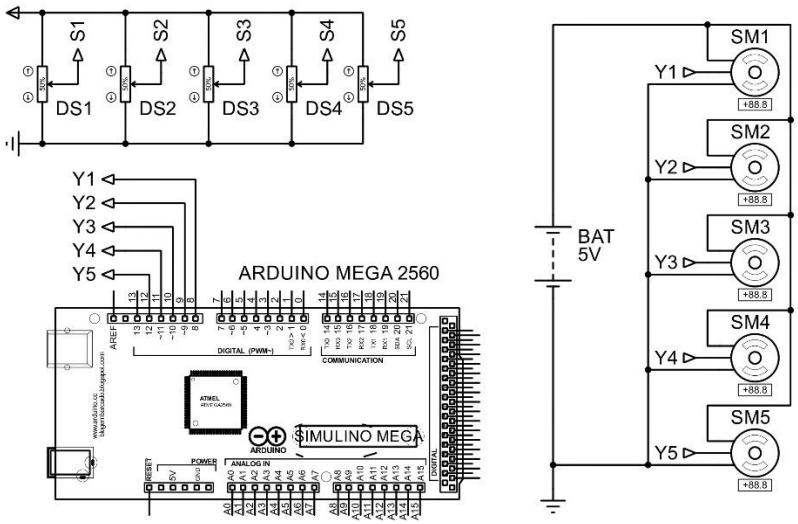

Figure 6.
Electronic diagram of the transradial prosthesis.

2.3. Central Composite Design

The proposed transradial prosthesis is capable of grasping a wide variety of objects with different shapes. To achieve this, an artificial neural network was used for parameter identification. Specifically, the neural network identifies the object's shape and determines the appropriate position of the prosthesis's fingers to grasp it. To train the artificial neural network and identify the parameters, a central composite design (CCD) was used, which allows for analyzing how a system's responses vary as a function of a set of input variables [23-25]. In this case, five independent variables corresponding to the distance sensor signals ($X_1, X_2, X_3, X_4, and\ X_5$) and five dependent variables corresponding to the servomotor positions ($Y_1, Y_2, Y_3, Y_4, and\ Y_5$) were considered. This type of experimental design considers combinations of high and low levels, as well as extreme levels and the midpoint of the independent variables, providing sufficient information to estimate a wide range of system responses to different input conditions. In this case, the transradial prosthesis was defined as being able to grasp objects with a minimum width of 1 cm and a maximum width of 9 cm. Table 1 shows the data used for training the artificial neural network. Using the CCD configurations, the ANN will be able to identify a greater number of objects, and the prosthesis will be able to grasp objects with regular and irregular shapes.

Table 1.
Configuration of the composite central design samples for ANN training.

Samples	X_1	X_2	X_3	X_4	X_5	Y_1	Y_2	Y_3	Y_4	Y_5
1	0.50	0.50	0.50	0.50	0.50	5.00	5.00	5.00	5.00	5.00
2	3.00	0.50	0.50	0.50	0.50	30.00	5.00	5.00	5.00	5.00
3	0.50	3.00	0.50	0.50	0.50	5.00	30.00	5.00	5.00	5.00
4	3.00	3.00	0.50	0.50	0.50	30.00	30.00	5.00	5.00	5.00
5	0.50	0.50	3.00	0.50	0.50	5.00	5.00	30.00	5.00	5.00
6	3.00	0.50	3.00	0.50	0.50	30.00	5.00	30.00	5.00	5.00
7	0.50	3.00	3.00	0.50	0.50	5.00	30.00	30.00	5.00	5.00
8	3.00	3.00	3.00	0.50	0.50	30.00	30.00	30.00	5.00	5.00
9	0.50	0.50	0.50	3.00	0.50	5.00	5.00	5.00	30.00	5.00
10	3.00	0.50	0.50	3.00	0.50	30.00	5.00	5.00	30.00	5.00
11	0.50	3.00	0.50	3.00	0.50	5.00	30.00	5.00	30.00	5.00
12	3.00	3.00	0.50	3.00	0.50	30.00	30.00	5.00	30.00	5.00
13	0.50	0.50	3.00	3.00	0.50	5.00	5.00	30.00	30.00	5.00
14	3.00	0.50	3.00	3.00	0.50	30.00	5.00	30.00	30.00	5.00
15	0.50	3.00	3.00	3.00	0.50	5.00	30.00	30.00	30.00	5.00
16	3.00	3.00	3.00	3.00	0.50	30.00	30.00	30.00	30.00	5.00
17	0.50	0.50	0.50	0.50	3.00	5.00	5.00	5.00	5.00	30.00
18	3.00	0.50	0.50	0.50	3.00	30.00	5.00	5.00	5.00	30.00
19	0.50	3.00	0.50	0.50	3.00	5.00	30.00	5.00	5.00	30.00
20	3.00	3.00	0.50	0.50	3.00	30.00	30.00	5.00	5.00	30.00
21	0.50	0.50	3.00	0.50	3.00	5.00	5.00	30.00	5.00	30.00
22	3.00	0.50	3.00	0.50	3.00	30.00	5.00	30.00	5.00	30.00
23	0.50	3.00	3.00	0.50	3.00	5.00	30.00	30.00	5.00	30.00
24	3.00	3.00	3.00	0.50	3.00	30.00	30.00	30.00	5.00	30.00
25	0.50	0.50	0.50	3.00	3.00	5.00	5.00	5.00	30.00	30.00
26	3.00	0.50	0.50	3.00	3.00	30.00	5.00	5.00	30.00	30.00
27	0.50	3.00	0.50	3.00	3.00	5.00	30.00	5.00	30.00	30.00
28	3.00	3.00	0.50	3.00	3.00	30.00	30.00	5.00	30.00	30.00
29	0.50	0.50	3.00	3.00	3.00	5.00	5.00	30.00	30.00	30.00
30	3.00	0.50	3.00	3.00	3.00	30.00	5.00	30.00	30.00	30.00
31	0.50	3.00	3.00	3.00	3.00	5.00	30.00	30.00	30.00	30.00
32	3.00	3.00	3.00	3.00	3.00	30.00	30.00	30.00	30.00	30.00
33	0.00	1.75	1.75	1.75	1.75	0.00	17.5	17.5	17.5	17.5
34	4.72	1.75	1.75	1.75	1.75	47.2	17.5	17.5	17.5	17.5
35	1.75	0.00	1.75	1.75	1.75	17.5	0.00	17.5	17.5	17.5
36	1.75	4.72	1.75	1.75	1.75	17.5	47.2	17.5	17.5	17.5
37	1.75	1.75	0.00	1.75	1.75	17.5	17.5	0.00	17.5	17.5
38	1.75	1.75	4.72	1.75	1.75	17.5	17.5	47.2	17.5	17.5
39	1.75	1.75	1.75	0.00	1.75	17.5	17.5	17.5	0.00	17.5
40	1.75	1.75	1.75	4.72	1.75	17.5	17.5	17.5	47.2	17.5
41	1.75	1.75	1.75	1.75	0.00	17.5	17.5	17.5	17.5	0.00
42	1.75	1.75	1.75	1.75	4.72	17.5	17.5	17.5	17.5	47.2
43	1.75	1.75	1.75	1.75	1.75	17.5	17.5	17.5	17.5	17.5
44	1.75	1.75	1.75	1.75	1.75	17.5	17.5	17.5	17.5	17.5

45	1.75	1.75	1.75	1.75	1.75	17.5	17.5	17.5	17.5	17.5
46	1.75	1.75	1.75	1.75	1.75	17.5	17.5	17.5	17.5	17.5

Figure 7 shows a graphical representation of some configurations proposed by the DDC, and how these are associated with the shape of objects or with the distance measured by the sensors placed on the fingers of the prosthesis. In this sense, the objects in the figure have a rigid shape (with straight sides), which is due to the characteristics of the CCD. However, these configurations will provide the artificial neural network with the ability to determine objects with curved shapes, as well as with sides that are neither horizontal nor vertical.

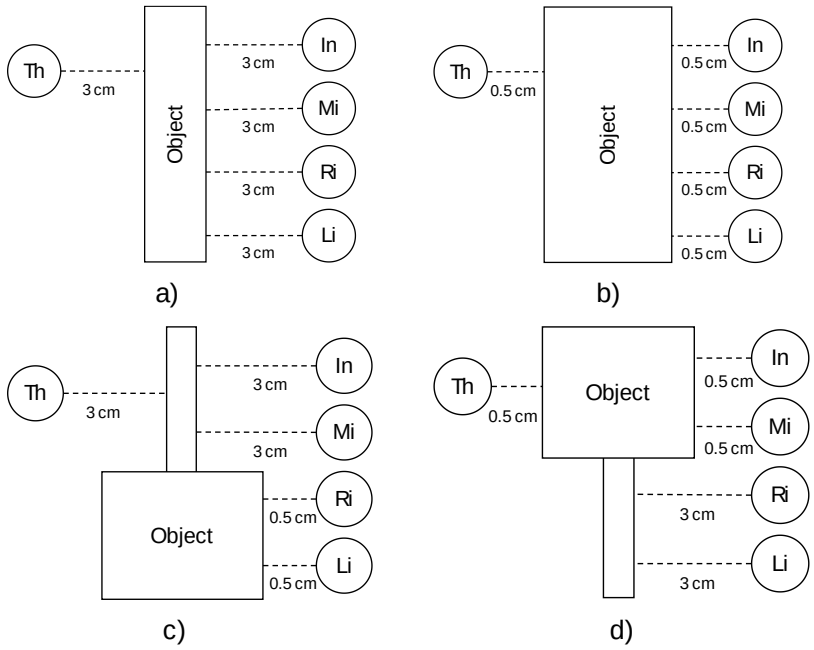

Figure 7.
Relationship of the DDC with the objects, a) sample 32, b) sample 1, c) sample 8, and d) sample 25.

2.4. Artificial Neural Network

Figure 8 shows the configuration of the artificial neural network used for object identification and grasping. As can be seen, the structure is composed of two intermediate layers: five signals in the input layer ($n = 5$), five neurons in the first intermediate layer ($n_1 = 5$), five neurons in the second intermediate layer ($n_2 = 5$), and five signals associated with the output layer ($n_3 = 5$). As mentioned previously, the network inputs are the readings from the distance sensors ($X_1, X_2, X_3, X_4, and\ X_5$), while the outputs correspond to the control signals for the five servomotors ($Y_1, Y_2, Y_3, Y_4, and\ Y_5$). The training or adjustment of the synaptic weights and thresholds of the artificial neural network is carried out by the backpropagation algorithm, which is a supervised algorithm that requires the desired value or result for each of the training samples (see data in Table 1) [26].

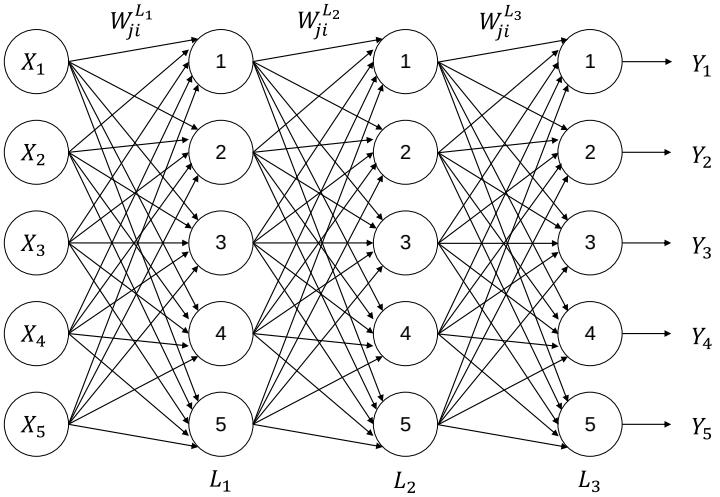

Figure 8.
Structure of the artificial neural network.

The backpropagation algorithm consists of two stages. The first is forward propagation, where the input variables flow from the input layer through the intermediate layers and into the output layer. In this context, Equation 1 represents the calculation of the total input of the j-th neuron in the first intermediate layer (L_1). This input is obtained as the weighted sum of the inputs X_i multiplied by their respective synaptic weights $W_{ji}^{(L_1)}$, where $W_{ji}^{(L_1)}$ is the weight connecting the j-th neuron in L_1 to the i-th input of the network. On the other hand, Equation 2 is used to determine the output of the j-th neuron in L_1, which is calculated by applying an activation function g(.) to the total input. This function must be differentiable throughout its domain. In this case, sigmoidal functions were used for all neurons in the network [27, 28].

$$I_j^{L_1} = \sum_{i=0}^{n} W_{ji}^{L_1} * X_i \quad (1)$$

$$Y_j^{L_1} = g\left(I_j^{L_1}\right) \quad (2)$$

In the second intermediate layer (L_2), the input and output of the j-th neuron are determined by Equations 3 and 4 respectively. In this case, the total input is the weighted sum of the outputs of L_1 multiplied by their respective synaptic weights $W_{ji}^{L_2}$, where $W_{ji}^{L_2}$ is the weight connecting the j-th neuron of L_2 and the i-th neuron of L_1.

$$I_j^{L_2} = \sum_{i=0}^{n_1} W_{ji}^{L_2} * Y_i^{L_1} \quad (3)$$

$$Y_j^{L_2} = g\left(I_j^{L_2}\right) \quad (4)$$

In the output layer (L_3), the input and output of the j-th neuron are determined by Equations 5 and 6 respectively. The total input is the weighted sum of the outputs of L_2 multiplied by their respective synaptic weights $W_{ji}^{L_3}$, where $W_{ji}^{L_3}$ is the weight connecting the j-th neuron of L_3 and the i-th neuron of L_2.

$$I_j^{L_3} = \sum_{i=0}^{n_2} W_{ji}^{L_3} * Y_i^{L_2} \quad (5)$$

$$Y_j^{L_3} = g\left(I_j^{L_3}\right) \quad (6)$$

Before applying the second stage of the backpropagation algorithm, a function must be used to measure the error between the responses produced by the network and the desired values. For this purpose, the squared error (SE) is used, calculated using Equation 7, which quantifies the difference between the predicted values ($Y_j^{L_3}$) and the desired values (d_j).

$$EC = \frac{1}{2}\sum_{i=0}^{n_3}\left(d_j - Y_j^{L_3}\right)^2 \quad (7)$$

The second stage of the backpropagation algorithm, known as backpropagation, consists of calculating the gradients down of the squared error (SE) with respect to the synaptic weights and thresholds. Where Equation 8 describes the calculation of the gradient down with respect to the synaptic weights in layer L_3, while Equation 9 is used for updating those weights.

$$W_{ji}^{L_3}(n+1) = W_{ji}^{L_3}(n) - \eta\frac{\partial EC}{\partial W_{ji}^{L_3}} \quad (8)$$

$$W_{ji}^{L_3}(n+1) = W_{ji}^{L_3}(n) - \eta\left(d_j - Y_j^{L_3}\right)\left(g'\left(I_j^{L_3}\right)\right)\left(Y_j^{L_2}\right) \quad (9)$$

And Equation 10 describes the calculation of the downward gradient with respect to the synaptic weights in the L_2 layer, while Equation 11 is used for updating said weights.

$$W_{ji}^{L_2}(n+1) = W_{ji}^{L_2}(n) - \eta\frac{\partial EC}{\partial W_{ji}^{L_2}} \quad (10)$$

$$W_{ji}^{L_2}(n+1) = W_{ji}^{L_2}(n) - \eta\left(\sum_{k=1}^{n_3}\left(d_k - Y_k^{L_3}\right)\left(g'\left(I_k^{L_3}\right)\right)\left(W_{ki}^{L_3}\right)\right)\left(g'\left(I_j^{L_2}\right)\right)\left(Y_j^{L_1}\right) \quad (11)$$

Equation 12 describes the calculation of the downward gradient with respect to the synaptic weights in the L_1 layer, while Equation 13 is used for updating said weights.

$$W_{ji}^{L_1}(n+1) = W_{ji}^{L_1}(n) - \eta\frac{\partial EC}{\partial W_{ji}^{L_1}} \quad (12)$$

$$W_{ji}^{L_1}(n+1) = W_{ji}^{L_1}(n) + \eta\left(\sum_{m=1}^{n_2}\left(\sum_{k=1}^{n_3}\left(d_k - Y_k^{L_3}\right)\left(g'\left(I_k^{L_3}\right)\right)\left(W_{ki}^{L_3}\right)\right)\left(g'\left(I_m^{L_2}\right)\right)\left(W_{mi}^{L_2}\right)\right)\left(g'\left(I_j^{L_1}\right)\right)\left(X_i\right) \quad (13)$$

The two stages of the backpropagation algorithm must be repeated for all data in the CCD, which constitutes an epoch. The total number of epochs required depends on how many are needed to achieve the desired accuracy or minimize the error of the artificial neural network. Finally, the efficiency of the artificial neural network was evaluated using the mean

squared error (MSE) and the root mean squared error (RMSE).

The former indicates the average deviation of the network's predictions from the expected values, while the latter indicates the deviation of the network from the expected values. This value is calculated with Equation 14 where s_1 is the number of samples in the dataset, Y_{ij} is the actual value of the j-th output of the i-th sample, and $\hat{Y}_{ij}$ is the value predicted by the network for that same output and sample.

$$MSE = \frac{1}{s_1}\sum_{i=1}^{s_1}\sum_{j=1}^{n_3}\left(Y_{ij} - \hat{Y}_{ij}\right)^2 \quad (14)$$

The implementation of the artificial neural network algorithm on the Arduino MEGA 2560 board yielded the following results: processing time of 5 milliseconds, and storage size of 13876 bytes. The general structure of the programming algorithm for object identification using the ANN is shown below.

```
// Define the samples of the CCD in a matrix.
// η=0.075; epochs=1000; samples=46; sample = 0; % epoch=0;
for k1=1:1: epochs
  for k=1:1:samples
    sample = sample +1;
    // Backpropagation algorithm: first stage
    // Current sample of X1, X2, …, X5.
    // Current desired signals D1, D2, …, D5.
    // Hidden layer 1 neurons: Use equations XX and YY
    // Hidden layer 2 neurons: Use equations XX and YY
    // Output layer neurons: use equations XX and YY
    // Squared error of the network: use equation XX1
    // Backpropagation algorithm: second stage
    // Update of W_i_j of the output layer: equation (XX)
    // Update of W_i_j of hidden layer 2: equation (XX)
    // Update of W_i_j of hidden layer 1: equation (XX)
  end
  epoch = epoch +1;
end
```

3. Results

To analyze the performance of the artificial neural network, the mean squared error (MSE) and root mean squared error (RMSE) were determined for each of its outputs, as well as the overall MSE and RMSE values considering all the network's outputs. Figure 9 shows the evolution of the network's overall MSE, as well as that of each of its outputs, as the number of epochs increases. As can be seen, at least 6000 epochs are required for each of the network's outputs to reach a minimum error level that allows for high precision, resulting in greater efficiency of the transradial prosthesis. Table 2 shows the obtained MSE and RMSE values. Another important aspect of these results is that they demonstrate that the proposed network structure fulfills its objective of correctly identifying the patterns derived from the shape of the objects.

Table 2.
Results obtained from the analysis of the artificial neural network.

Output	MSE (°)	RMSE (°)
General	2.9043	1.7042
Y_1	0.4366	0.6607
Y_2	0.4867	0.6976
Y_3	0.3700	0.6082
Y_4	1.2283	1.1082
Y_5	0.3826	0.6185

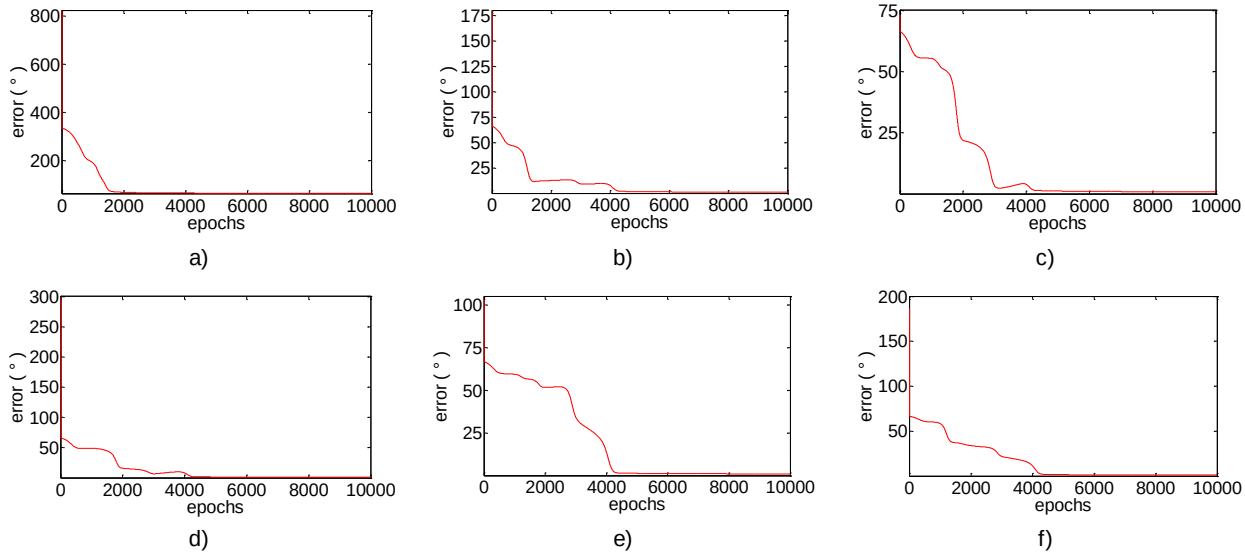

Figure 9.
Evolution of the mean squared error, a) general of the network, b) output Y_1, c) output Y_2, d) output Y_3, e) output Y_4 and f) output Y_5.

To demonstrate the network's efficiency in identifying object shapes and the appropriate gripping technique, simulation tests were performed to analyze the artificial neural network's performance. Table 3 presents the network's responses, or the angles each finger must move to grasp the object, based on the distances measured by the distance sensors. Figure 10 shows a graphical representation of the simulation tests described in Table 3 specifically the initial position of each finger (circles) and the distance measured by the sensors relative to the shape (square, triangle, hexagon, and circle).

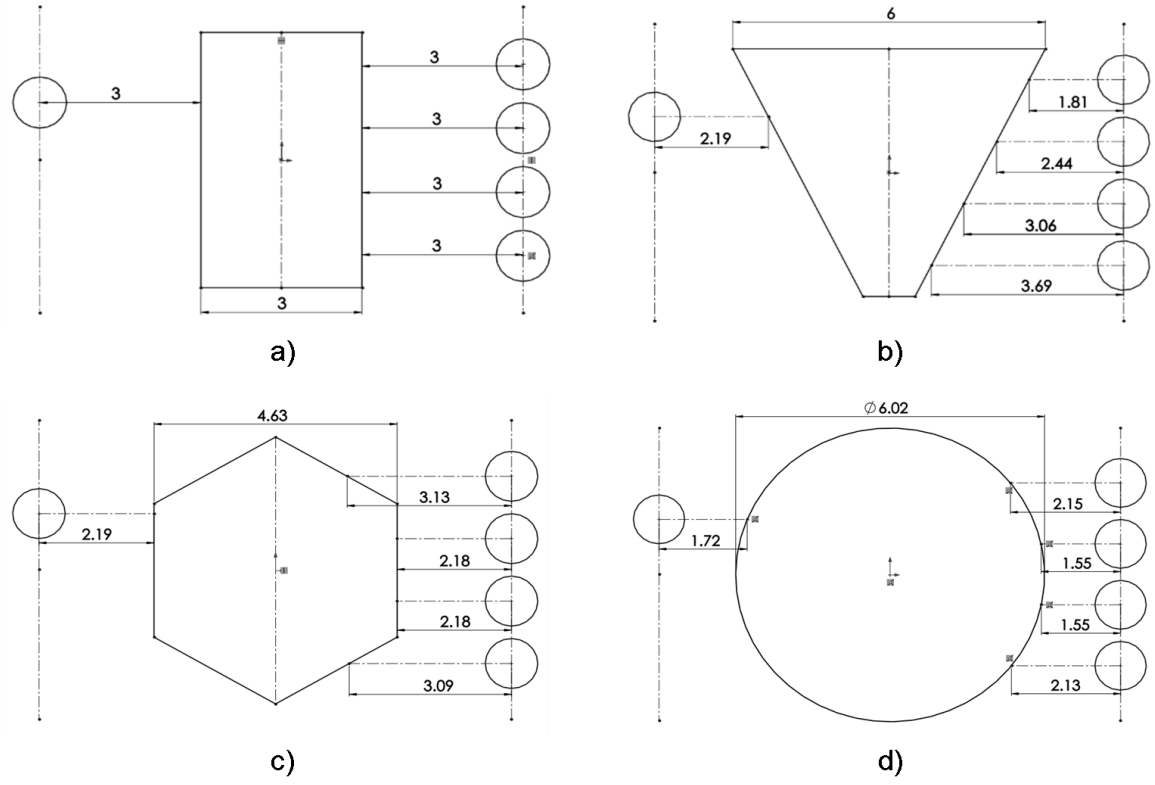

Figure 10.
Graphical representation of the configurations in Table 3.

Table 3.
Results of object identification with the artificial neural network.

Object	X_1	X_2	X_3	X_4	X_5	Y_1	Y_2	Y_3	Y_4	Y_5
Square	3.00	3.00	3.00	3.00	3.00	32.121	31.852	31.579	32.189	31.34
Triangle	2.19	1.18	2.44	3.06	3.69	21.936	10.376	24.027	32.802	36.319
Hexagon	2.19	3.13	2.18	2.18	3.09	24.292	37.049	24.181	22.251	36.029
Circle	1.72	2.15	1.55	1.55	2.13	17.355	24.449	15.052	13.577	24.032

Figure 11 shows how the prosthesis grips a polygonal object measuring 8 cm wide, 5.5 cm high, and weighing 300 g. In this case, the finger position on the object was appropriate, as the fingertips made contact with the object's surface. Therefore, it can be concluded that the proposed transradial prosthesis is a viable solution for individuals who have lost a forearm transradially. Table 4 presents a comparative analysis that considers various technical aspects of several transradial prosthesis prototypes, which have been previously proposed in the scientific literature. This comparison focuses specifically on the materials used for their construction, as well as the advantages and disadvantages related to their durability, ease of implementation, and control system. The purpose of including this table is to provide a clear and systematic overview of the main characteristics that differentiate the existing prototypes, allowing for the identification of common patterns and potential areas for improvement in future developments. Based on the comparative analysis, it is concluded that the proposed system represents a more efficient alternative from a construction standpoint. Furthermore, it incorporates an artificial neural network that operates with a high degree of accuracy in both object identification and the selection of the appropriate method for holding them. This network has been designed to operate efficiently on low-cost platforms, which reinforces the project's economic viability. Thanks to this combination of structural simplicity, low cost, and high operational efficiency, the proposed prosthesis is positioned as an innovative option.

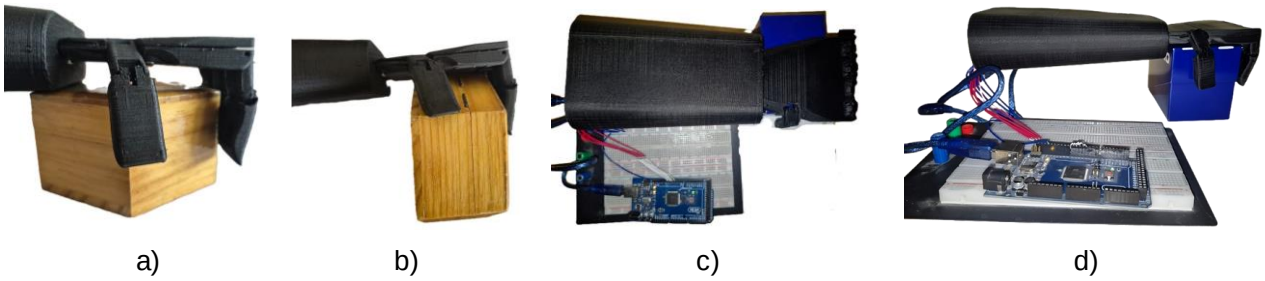

Figure 11.
Object clamping with the transradial prosthesis, a) test 1, b) test 2, c) test 3 and d) test 4.

Table 4.
Comparison between the developed prosthesis and the latest generation of commercial prostheses.

Name	Features
A 3D-Printed EEG based Prosthetic Arm Fuentes-Gonzalez, et al. [29].	A transradial prosthesis was developed using Blender software for dimensioning. All prosthetic components were 3D printed using PLA. Three actuators connected to the fingers via nylon thread were incorporated, along with a device capable of measuring brain electrical signals. This device is equipped with a frontal sensor, wireless data transmission, and a control unit for EEG signal acquisition. The EEG data obtained was filtered and adjusted to the patient's capabilities. Finally, the prosthesis can open and close the hand with a force of 11.0 N, sufficient for grasping objects used in daily life.
A Proposal of Bioinspired Soft Active Hand Prosthesis Toro-Ossaba, et al. [30].	This article presents a transradial prosthesis with a design that mimics the musculoskeletal components and morphology of the human hand. CAD models were developed, and a 3D printer was used to fabricate the prosthesis's skeletal structure; soft materials were used for the musculoskeletal components. A myoelectric control system based on five EMG sensors and a recurrent neural network was implemented to classify hand gestures. With this system, the prosthesis was able to intuitively perform five different gestures, achieving 87% accuracy.
Continuous Semi-autonomous Prosthesis Control Using a Depth Sensor on the Hand Castro and Dosen [31].	This article describes the implementation of a control system for a prosthesis that utilizes myoelectric sensors, a depth sensor located on the dorsal side of the hand, and proportional control. The system identifies the grip type, object size and orientation, and the necessary wrist rotation to manipulate objects of varying shapes, sizes, and orientations, whether placed individually or in unstructured environments. The prosthesis has two degrees of freedom: it can rotate the wrist and perform two types of grips by opening and closing the fingers. For control, two dual-differential surface electrodes were placed on the user's right forearm, along with a camera located on the dorsal side of the prosthetic hand. A laptop computer and a Bluetooth connection were used to integrate and coordinate all system elements. Experimental results demonstrated that participants successfully used the system to manipulate a wide variety of objects and components.
This work	This paper presents a transradial prosthesis designed for gripping objects of various shapes (cylindrical, spherical, rectangular, square, etc.). Distance sensors were used to record object information, and servomotors were used to adjust the position of the prosthesis's

	fingers. An artificial neural network was also employed to identify object patterns and characteristics and determine the appropriate gripping mode. The network was trained using a central composite design, which provided effective modeling and accurate identification of patterns corresponding to different objects. The prosthesis was developed using a Creality CR-5 Pro H 3D printer with PLA carbon fiber filament. The control system was implemented on an Arduino MEGA board, and distance sensors were used instead of myoelectric sensors to avoid the problems associated with myoelectric signals.

4. Discussion

The results show that applying an artificial neural network to a transradial prosthesis allows for the identification of the characteristics of objects with different shapes (spherical, circular, square, triangular, etc.), as well as determining the appropriate way to grasp them with the prosthesis. Likewise, the use of an experimental design (specifically, the central composite design) provided samples with the appropriate characteristics for the correct identification of objects with regular and irregular shapes. This is because the samples generated by the central composite design are composed of combinations of the maximum and minimum values, as well as the midpoint and extreme values of the system's independent variables (response of the distance sensors). These results show that it is possible to design and develop transradial prostheses capable of performing movements based on the shape of objects, in contrast to most current prostheses of this type, which only allow for some gestures or opening and closing the wrist to grasp objects. This demonstrates that the quality of the samples used to train the artificial neural network is a fundamental aspect for the proper functioning of the prosthesis.

5. Conclusions

In this work, a transradial prosthesis capable of grasping objects with regular and irregular shapes was designed and developed. A methodology is presented that increases the gripping modes and the variety of objects the device can manipulate. To identify the shape of the objects, an artificial neural network trained with data obtained from five distance sensors located on the fingers of the prosthesis was used. From this information, the network determines the appropriate movement that five servomotors must perform to adjust the position of the fingers and grasp the object correctly. One of the most important aspects in the design of a transradial prosthesis is the number of shapes it can grasp. Therefore, a central composite design was used to plan a set of tests (observations), in which each combination proposed by the experimental design was associated with the desired movement of the prosthesis fingers. This strategy avoids the use of random combinations or tests with arbitrarily selected objects and allows for the extraction and analysis of the relevant characteristics of each object for their subsequent application in the artificial neural network.

Another important aspect that improved the efficiency of the transradial prosthesis was the artificial neural network's ability to map systems with multiple inputs and outputs, as well as its ability to identify patterns from a set of samples. In this regard, the artificial neural network was able to recognize objects with square, circular, triangular, hexagonal, and other shapes. These characteristics can contribute to the development of more functional and advanced prostheses than current ones, which generally only allow finger gestures and opening or closing the wrist to grasp objects. However, it is still necessary to improve the aesthetics and ergonomics of the proposed transradial prosthesis, as these aspects are fundamental for people who have lost an arm. Likewise, mechanical design should be optimized, primarily through the implementation of servomotors that allow for the manipulation of heavier objects. Future studies should explore new methodologies that expand the functions of transradial prostheses. Furthermore, these prostheses must be designed with advanced materials that improve both user comfort and aesthetic appearance, making them thinner and more flexible to more realistically mimic the human arm.

References

[1] T. Motahar and J. Wiese, "A review of personal informatics research for people with motor disabilities," *Proceedings of the ACM on Interactive, Mobile, Wearable and Ubiquitous Technologies*, vol. 6, no. 2, pp. 1-31, 2022. https://doi.org/10.1145/3534614

[2] G. Soghoyan, A. Biktimirov, Y. Matvienko, I. Chekh, M. Sintsov, and M. A. Lebedev, "Peripheral nerve stimulation enables somatosensory feedback while suppressing phantom limb pain in transradial amputees," *Brain Stimulation*, vol. 16, no. 3, pp. 756-758, 2023.

[3] V. Mendez, F. Iberite, S. Shokur, and S. Micera, "Current solutions and future trends for robotic prosthetic hands," *Annual Review of Control, Robotics, and Autonomous Systems*, vol. 4, no. 1, pp. 595-627, 2021. https://doi.org/10.1146/annurev-control-071020-104336

[4] P. Weiner, J. Starke, S. Rader, F. Hundhausen, and T. Asfour, "Designing prosthetic hands with embodied intelligence: The KIT prosthetic hands," *Frontiers in Neurorobotics*, vol. 16, p. 815716, 2022. https://doi.org/10.3389/fnbot.2022.815716

[5] C. Gentile, F. Cordella, and L. Zollo, "Hierarchical human-inspired control strategies for prosthetic hands," *Sensors*, vol. 22, no. 7, p. 2521, 2022. https://doi.org/10.3390/s22072521

[6] Z. Chen, H. Min, D. Wang, Z. Xia, F. Sun, and B. Fang, "A review of myoelectric control for prosthetic hand manipulation," *Biomimetics*, vol. 8, no. 3, p. 328, 2023. https://doi.org/10.3390/biomimetics8030328

[7] J. O. d. O. de Souza, M. D. Bloedow, F. C. Rubo, R. M. de Figueiredo, G. Pessin, and S. J. Rigo, "Investigation of different approaches to real-time control of prosthetic hands with electromyography signals," *IEEE Sensors Journal*, vol. 21, no. 18, pp. 20674-20684, 2021. https://doi.org/10.1109/JSEN.2021.3099744

[8] A. Prakash and S. Sharma, "A low-cost transradial prosthesis controlled by the intention of muscular contraction," *Physical and Engineering Sciences in Medicine*, vol. 44, no. 1, pp. 229-241, 2021. https://doi.org/10.1007/s13246-021-00972-w

[9] Z. Koudelkova *et al.*, "Verification of finger positioning accuracy of an affordable transradial prosthesis," *Designs*, vol. 7, no. 1, p. 14, 2023.

[10] B. Fang *et al.*, "Simultaneous sEMG recognition of gestures and force levels for interaction with prosthetic hand," *IEEE Transactions on Neural Systems and Rehabilitation Engineering*, vol. 30, pp. 2426-2436, 2022. https://doi.org/10.1109/TNSRE.2022.3199809

[11] R. Tchantchane, H. Zhou, S. Zhang, and G. Alici, "A review of hand gesture recognition systems based on noninvasive wearable sensors," *Advanced Intelligent Systems*, vol. 5, no. 10, p. 2300207, 2023. https://doi.org/10.1002/aisy.202300207

[12] R. Brack and E. H. Amalu, "A review of technology, materials and R&D challenges of upper limb prosthesis for improved user suitability," *Journal of Orthopaedics*, vol. 23, pp. 88-96, 2021. https://doi.org/10.1016/j.jor.2020.12.009

[13] M. G. Abdolrasol *et al.*, "Artificial neural networks based optimization techniques: A review," *Electronics*, vol. 10, no. 21, p. 2689, 2021. https://doi.org/10.3390/electronics10212689

[14] C. G. Villegas-Mier, J. Rodriguez-Resendiz, J. M. Álvarez-Alvarado, H. Rodriguez-Resendiz, A. M. Herrera-Navarro, and O. Rodríguez-Abreo, "Artificial neural networks in MPPT algorithms for optimization of photovoltaic power systems: A review," *Micromachines*, vol. 12, no. 10, p. 1260, 2021. https://doi.org/10.3390/mi12101260

[15] J. Kufel *et al.*, "What is machine learning, artificial neural networks and deep learning?—Examples of practical applications in medicine," *Diagnostics*, vol. 13, no. 15, p. 2582, 2023. https://doi.org/10.3390/diagnostics13152582

[16] C. Lu, S. Li, and Z. Lu, "Building energy prediction using artificial neural networks: A literature survey," *Energy and Buildings*, vol. 262, p. 111718, 2022. https://doi.org/10.1016/j.enbuild.2021.111718

[17] K. S. Garud, S. Jayaraj, and M. Y. Lee, "A review on modeling of solar photovoltaic systems using artificial neural networks, fuzzy logic, genetic algorithm and hybrid models," *International Journal of Energy Research*, vol. 45, no. 1, pp. 6-35, 2021. https://doi.org/10.1002/er.5608

[18] L. H. S. Sales De Menezes *et al.*, "Artificial neural network hybridized with a genetic algorithm for optimization of lipase production from Penicillium roqueforti ATCC 10110 in solid-state fermentation," *Biocatalysis and Agricultural Biotechnology*, vol. 31, p. 101885, 2021. https://doi.org/10.1016/j.bcab.2020.101885

[19] A. Hosney, S. Ullah, and K. Barčauskaitė, "A review of the chemical extraction of chitosan from shrimp wastes and prediction of factors affecting chitosan yield by using an artificial neural network," *Marine Drugs*, vol. 20, no. 11, p. 675, 2022. https://doi.org/10.3390/md20110675

[20] J. Purdum, *Beginning C for arduino*. Berkeley, CA: Apress, 2015.

[21] D. J. Russell, *Introduction to arduino*. Cham: Springer, 2010.

[22] C. Bell, *Arduino programming," in beginning IoT projects*. Berkeley, CA: Apress, 2021.

[23] M. Gregor, P. Grznar, S. Mozol, and L. Mozolova, "Design of simulation experiments using central composite design," *Acta Simulatio*, vol. 9, no. 2, pp. 21-25, 2023. https://doi.org/10.22306/asim.v9i2.99

[24] S. Bhattacharya, "Central composite design for response surface methodology and its application in pharmacy." London, United Kingdom: IntechOpen, 2021.

[25] S. Somadasan, G. Subramaniyan, M. S. Athisayaraj, and S. K. Sukumaran, "Central composite design: An optimization tool for developing pharmaceutical formulations," *Journal of Young Pharmacists*, vol. 16, no. 3, pp. 400-409, 2024. https://doi.org/10.5530/jyp.2024.16.52

[26] R. Kumar, S. Srivastava, J. Gupta, and A. Mohindru, "Comparative study of neural networks for dynamic nonlinear systems identification," *Soft Computing*, vol. 23, no. 1, pp. 101-114, 2019. https://doi.org/10.1007/s00500-018-3235-5

[27] O. A. Montesinos López, A. Montesinos López, and J. Crossa, *Fundamentals of artificial neural networks and deep learning*. Cham: Springer International Publishing, 2022.

[28] I. N. Da Silva, D. Hernane Spatti, R. Andrade Flauzino, L. H. B. Liboni, and S. F. Dos Reis Alves, *Artificial neural networks*. Cham: Springer International Publishing, 2017.

[29] J. Fuentes-Gonzalez, A. Infante-Alarcon, V. Asanza, and F. R. Loayza, "A 3D-printed EEG based prosthetic arm," presented at the IEEE International Conference on E-health Networking, Application & Services (HEALTHCOM), IEEE, 2021.

[30] A. Toro-Ossaba, J. C. Tejada, S. Rúa, and A. López-González, "A proposal of bioinspired soft active hand prosthesis," *Biomimetics*, vol. 8, no. 1, p. 29, 2023. https://doi.org/10.3390/biomimetics8010029

[31] M. N. Castro and S. Dosen, "Continuous semi-autonomous prosthesis control using a depth sensor on the hand," *Frontiers in Neurorobotics*, vol. 16, p. 814973, 2022. https://doi.org/10.3389/fnbot.2022.814973